potential analysis to have the parameters given in Table I under $\lambda=1$. Evaluation of the R function for the potential parameters at $E_n=2$ MeV (c.m.) gives $R_{2\frac{1}{2}}(2\text{ MeV})=-0.583$. Thus the background term assumed in the fitting provides a reasonable simulation of the sum of the resonance term and the background found from the potential analysis.

The results of these calculations would seem to indicate that the potential-well analysis used here is of value. By using this scheme, it would seem that background contributions can be reasonably well determined in an *a priori* manner and that only compound resonance parameters need be fitted. This eliminates several of the parameters needed in the fitting procedure and, therefore, reduces somewhat the ambiguity of the parameters found. However, a diffuse-well calculation is expected to give better agreement with the data.

ACKNOWLEDGMENTS

The authors wish to thank Dr. A. J. Elwyn, Dr. A. Langsdorf, Jr., and Dr. F. P. Mooring for their valuable collaboration in performing the experiment. The authors are particularly indebted to Frank Dunnill for rewriting the program COMBO to automatically plot the many calculated and experimental results, without which the completion of this work would not have been possible.

PHYSICAL REVIEW VOLUME 188, NUMBER 4 20 DECEMBER 1969

Experimental Investigations of the $C^{12}(h, p)N^{14}$ Reaction Mechanism

F. HAAS, B. HEUSCH, A. GALLMANN, AND D. A. BROMLEY*

Laboratoire de Physique Nucléaire et d'Instrumentation Nucléaire, Strasbourg, France

(Received 9 June 1969)

Systematic studies on proton angular distribution and proton–γ-radiation angular correlations have been carried out on the $C^{12}(h, p)N^{14}$ reaction throughout the energy range $4.62\leq E_h\leq 11.0$ MeV. ($h\equiv He^3$.) Both direct and compound-system reaction amplitudes are present; however, the latter appear to dominate. Striking resonant phenomena are observed, and it is suggested that these correspond to quasigiant resonances in the excitation-energy range from 17 to 23 MeV in O^{15} having a particularly simple structure involving single-proton orbitals coupled to excited N^{14} core configurations. A systematic correlation has been observed between the population of $|m|=1$ magnetic substates of the 7.03-MeV state in the residual nucleus and the appearance of backward peaking in the corresponding proton angular distributions. A crude argument relating these phenomena to the participation of a heavy-particle direct stripping mechanism is suggested.

I. INTRODUCTION

ALTHOUGH extensive studies have been reported (see Ref. 1 for a review of all work prior to 1960 and detailed references of this work) on the mechanism for reactions induced by He^3 nuclei (henceforth *helions*, h)[2] on light nuclei, relatively little unambiguous information has been obtained. Even at low bombarding energies, the high helion mass excess (14.93 MeV) results in high compound-system energies, typically $\sim$20 MeV, so that isolated compound-resonance phenomena are not anticipated: Moreover, it has been demonstrated that in many of the reactions studied, direct reaction amplitudes play an important, if not dominant, role.

Examination of the compound-system binding energies for helions incident on light targets[1] shows three somewhat anomalous cases. In the Be^7 compound system, the helion binding energy is only 1.58 MeV; at low helion energies, no compound states are accessible and the reaction proceeds by direct capture. In the Ne^{19} compound system, the helion binding energy is next lowest at 8.42 MeV; studies on this system, and particularly on the $O^{16}(h, \alpha)O^{15}$ reaction, did successfully isolate and study resonances in the Ne^{19} system,[3] but to date this is the only such example in helion studies. The next lowest binding energy is that in O^{15} (12.12 MeV), corresponding to helion bombardment of a C^{12} target. In the hope of finding a situation amenable to detailed reaction mechanism study at the relatively low energies ($E_h\lesssim 11$ MeV) available for this work, and on the basis of the availability of much previous data on this reaction from this laboratory, and elsewhere, we have concentrated on the $C^{12}(h, p)N^{14}$ interaction.

The earliest measurements on this reaction at low energies[4] demonstrated clearly that even for $E_h\leq 3$

* Permanent address: Wright Nuclear Structure Laboratory, Yale University, New Haven, Conn. 06520.

[1] D. A. Bromley and E. Almqvist, in *Reports on Progress in Physics* (The Physical Society, London, 1960), Vol. 23, p. 544ff. See this review for detailed referencing of all earlier work on helion reactions.

[2] See, for example, Proceedings of the Tokyo Symposium on Helium 3 Reactions, Tokyo, 1968, edited by K. Matsuda (unpublished).

[3] D. A. Bromley, J. A. Kuehner, and E. Almqvist, Nucl. Phys. **13**, 1 (1959).

[4] D. A. Bromley, E. Almqvist, H. E. Gove, A. E. Litherland, E. B. Paul, and A. J. Ferguson, Phys. Rev. **105**, 957 (1957).

MeV, both direct and compound-system amplitudes were important, although striking resonant structure was observed in some of the excitation functions. No extraction of specific resonance parameters has appeared feasible, however, in contrast to the situation in Ne^{19}.[3] More recent detailed studies have spanned the range in helion energy to 25.3 MeV[5]; perhaps the most recent such work was carried out at 20.1 MeV,[6] where it was found possible to obtain a reasonable reproduction of the experimental data using a distorted-wave analysis based on a spin-independent interaction potential and realistic shell-model wave functions[7,8] for the N^{14} states populated.

In an earlier paper from this laboratory,[9] we noted that at 8.92- and 5.11-MeV helion energies, in Litherland and Ferguson method-II correlation geometry,[10] there occurred a striking change in the relative population of the accessible magnetic substates of the 2^+, $T=0$, 7.03-MeV state in N^{14}. On the basis of the early angular distribution measurements for the corresponding proton group, at helion energies in the 8–9-MeV range, there appeared to be a marked correlation between population of the $|m|=1$ substate and pronounced backward peaking in the corresponding proton angular distribution. In this paper, we present the results of a more extensive investigation of these phenomena. Earlier work,[11] in the range $5.7 \leq E_h \leq 10.23$ MeV, which was concentrated primarily on forward angle distributions in the hope of obtaining nuclear spectroscopic information on N^{14}, nonetheless indicated pronounced fluctuation of the extreme backward angle differential cross sections.

We here report on a systematic study not only of the magnetic substate population variation of the 7.03-MeV residual state with incident helion energy, but also the variation of the proton angular distribution shapes and total reaction cross sections for all residual N^{14} states up to and including that at 7.03 MeV as functions of the incident energy in the range $4.62 \leq E_h \leq 11.0$ MeV.

Striking resonant effects have been found indicating the importance of compound-system effects; on the other hand, the angular distributions, at certain energies, exhibit typical direct interaction behavior. We present a discussion of these results utilizing the well-established shell-model wave functions[7,8] for the final N^{14} states and the C^{12} target state involved. We suggest that some of the striking differences in the total cross-section excitation functions for the dominant $(p_{3/2}, p_{1/2})^{-1}$ states may reflect selection rule and two-particle fractional parentage considerations, that the systematic variation of the magnetic substate populations may reflect the presence of quasigiant resonances in O^{15} having particularly simple structure and consequent overlap with the particular residual state (7.03 MeV) studied; and that the correlation between population of $|m|=1$ substates in this final state and backward peaking in the corresponding angular distribution may reflect a simple mechanical argument based on an assumed pronounced oblate deformation of the C^{12} target.

II. EXPERIMENTAL APPROACH

A standard scattering chamber, 34.4 cm in diameter, has been utilized in measurements of the angular distributions and the excitation functions. Both commercial (ORTEC) and locally fabricated semiconductor detectors have been used with standard modular electronic systems. Effective energy resolutions of 22–25 keV were obtained typically under beam conditions; when aluminum absorbers of 15–30 μ were used to remove α particles and scattered helions from the output particle spectra, the resolution deteriorated to 40–50 keV. The target foils were 40 $\mu g/cm^2$ in areal density, self-supporting, and of natural isotopic constituency.

The helion beam in the energy range up to 11 MeV was obtained from the Strasbourg 5.5-MV HVEC Van de Graaff accelerator equipped for acceleration of doubly ionized helium beams. Beam currents were typically of the order of 100 nA.

Two separate measurements were carried out on the back-angle excitation functions ($\theta_{lab}=172°$): In the first, no absorber was used and the range $4.0 \leq E_h \leq 11.0$ MeV was scanned in 500-keV steps; in the second, a 20-μ aluminum absorber was installed and the range $5.0 \leq E_h \leq 11.0$ MeV was again scanned, but in steps of between 100 and 200 keV in energy. From comparison of these two sets of data, it was possible to disentangle the desired proton-excitation-curve data and exclude other charged particle groups. All of the excitation-function data have been normalized to an effective 100 μC of helion beam charge delivered to a shielded Faraday cage some 2 m beyond the target center.

Angular distributions for proton groups feeding states in N^{14} up to 7.03 MeV in excitation were measured at 20 helion energies in the range covered by the excitation curves above. In each case, a fixed 90° monitor counter was used in monitoring target condition through comparison with integrated beam readings; the absolute cross sections were obtained by normalizing the back-angle data ($\theta_{lab}=172°$) to the excitation-curve data. In these angular distributions, attention was focused on backward angles and, in as much as other data exist on the forward-angle regions, we have taken only the relatively few forward-angle

[5] K. Matsuda, N. Nakanishi, S. Takeda, and T. Wada, J. Phys. Soc. Japan **25**, 1207 (1968).
[6] N. F. Mangelson, B. G. Harvey, and N. K. Glendenning, Nucl. Phys. **A117**, 161 (1968).
[7] W. W. True, Phys. Rev. **130**, 1530 (1963).
[8] S. Cohen and D. Kurath, Nucl. Phys. **73**, 1 (1965); D. Kurath (private communication).
[9] A. Gallmann, F. Haas, and B. Heusch, Phys. Rev. **164**, 1257 (1967).
[10] A. Litherland and A. J. Ferguson, Can. J. Phys. **39**, 788 (1961).
[11] S. Hinds and R. Middleton, Proc. Phys. Soc. (London) **55**, 745 (1959).

TABLE I. Comparison of total reaction cross sections in the $C^{12}(h, p)N^{14}$ reaction as studied for $5.0 \leq E_h \leq 11.0$ MeV and at $E_h = 20.1$ MeV.

Residual N^{14} level excitation	$J^\pi T$	Average total cross section (mb) $5.0 \leq E_h \leq 11.0$ MeV	Total cross section (mb) $E_h = 20.1$ MeV $10° \leq \theta \leq 70°$	Total cross section (mb) $E_h = 25.3$ MeV $15° \leq \theta \leq 130°$
7.03	2^+0	22	0.84	1.05
6.44	3^+0	80	10.80	7.75
6.21	1^+0	47	2.83	2.24
5.83	3^-0	53	1.58	2.09
5.69	1^-0	43	1.84	1.22
5.10	2^-0	55	3.35	3.04
4.91	0^-0	23	1.34	0.84
3.95	1^+0	37	1.41	1.51
2.31	0^+1	NA	0.77	1.04
0	0^+1	NA	0.96	1.37

measurements sufficient to delineate the general behavior and to provide a reliable total cross-section measurement. At certain angles, extraction of reaction α particle and scattered helion groups has increased the effective probable errors in the proton measurements, but in no case does this affect any of our conclusions.

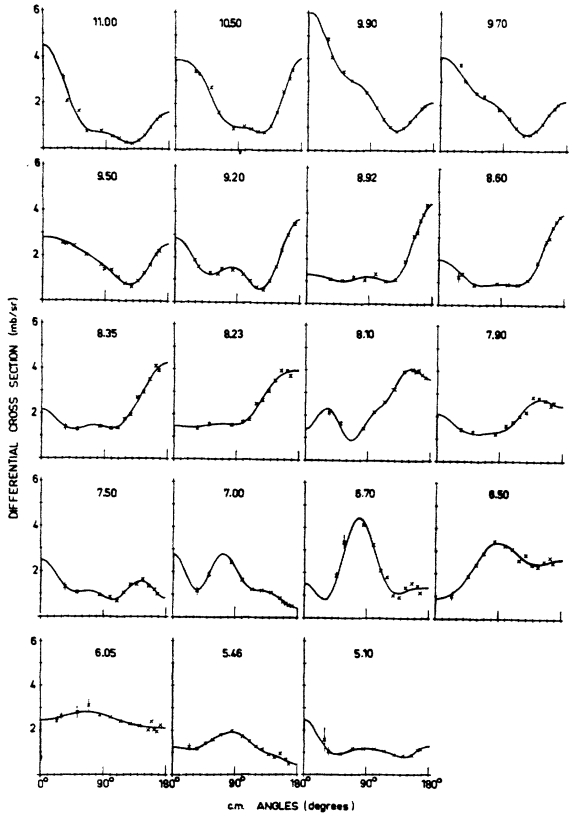

FIG. 1. Proton angular distributions from the $C^{12}(h, p_9)N^{14*}$ reaction (7.03-MeV state) measured in the 5.10–11.0-MeV helion energy range. The solid line is the best fit obtained with a Legendre polynomial expansion via a least-squares calculation.

All angular distribution data were reduced and fitted to the usual Legendre polynominal expansion via a least-squares program utilizing the laboratory IBM 1130 computer. In each case, to avoid spurious fitting, an assumed zero-degree intensity, with large assigned error, was included with the experimental data, and fits were obtained to expansions of variable maximum Legendre polynomial order up to and including eight; this limit being set by the fact that angular distributions contained input data at only 16 separate angles.

In our selection of the assumed zero-degree data, we have been guided by the earlier published multigap-spectrograph data where these are available.

The experimental system used in the correlation

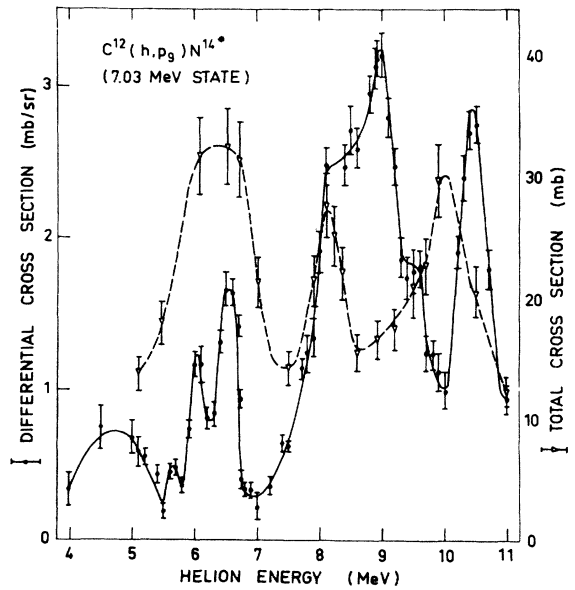

FIG. 2. Differential cross section (solid line and ● points) at a laboratory angle of 172° and total cross section (dashed line and ▽ points) of the proton group from the $C^{12}(h, p_9)N^{14*}$ reaction (7.03-MeV state).

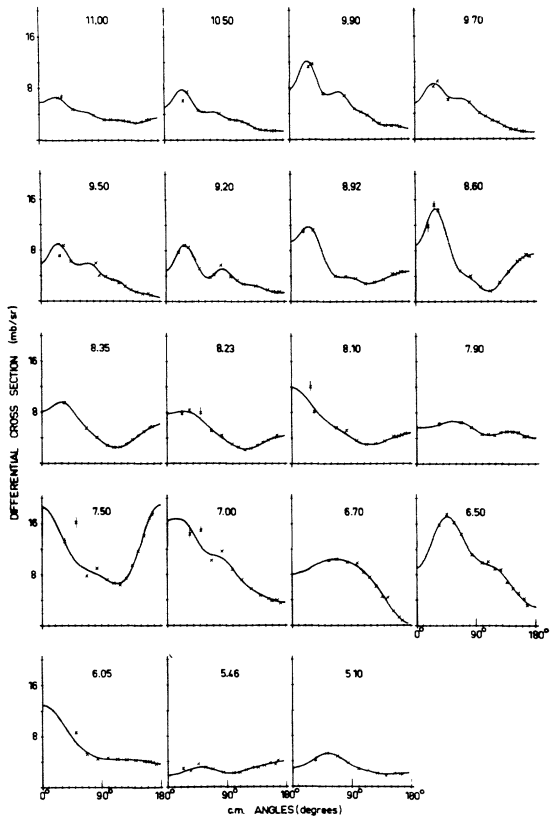

FIG. 3. Proton angular distributions from the $C^{12}(h, p_8)N^{14*}$ reaction (6.44-MeV state) measured in the 5.10–11.0-MeV helion energy range. The solid line is the best fit obtained with a Legendre polynomial expansion via a least-squares calculation.

studies has been described previously[12,13] and is now standard for use in the method-II Litherland and Ferguson geometry. As here used, γ radiation was detected simultaneously in three 5×6 in. standard NaI (Tl) spectrometers, each feeding a separate 4096-channel analyzer; this had the obvious advantage of increased efficiency and the perhaps less obvious advantage of greatly simplifying normalization questions. Standard modular electronics were utilized with crossover pickoff timing and a coincidence resolving time of approximately 60 nsec.

In the present series of measurements, correlation data were accumulated at 17 energies in the range $6.0 \leq E_h \leq 11.0$ MeV; these are in addition to those previously acquired for $4.62 \leq E_h \leq 5.46$ MeV and at $E_h = 8.92$ MeV.

Unfortunately, the available instrumentation did not permit simultaneous study of proton-γ correlations involving all the residual levels in N^{14} at a given time because of the number of channels required to yield adequate energy resolution for each. As we shall note below, such measurements will be completed here in the near future.

III. EXCITATION FUNCTIONS AND ANGULAR DISTRIBUTIONS

We shall present the data on excitation functions, angular distributions, and total cross sections for each level in N^{14} systematically, beginning with the highest excitation studied. The total cross-section data were obtained from the normalization to the $\theta_{lab} = 172°$ excitation-function data and the subsequent Legendre polynomial fits. The detailed Legendre polynomial coefficients are available on request from the authors but will not be included herein; the curves in the appropriate angular distribution figures correspond to these polynomial fits. In listing each residual level in the presentation below, we shall include its J^π, T assignment and its assumed dominant shell-model wave function.

In Table I, we compare the "average" total cross sections in the range $5.0 \leq E_h \leq 11.0$ MeV with data

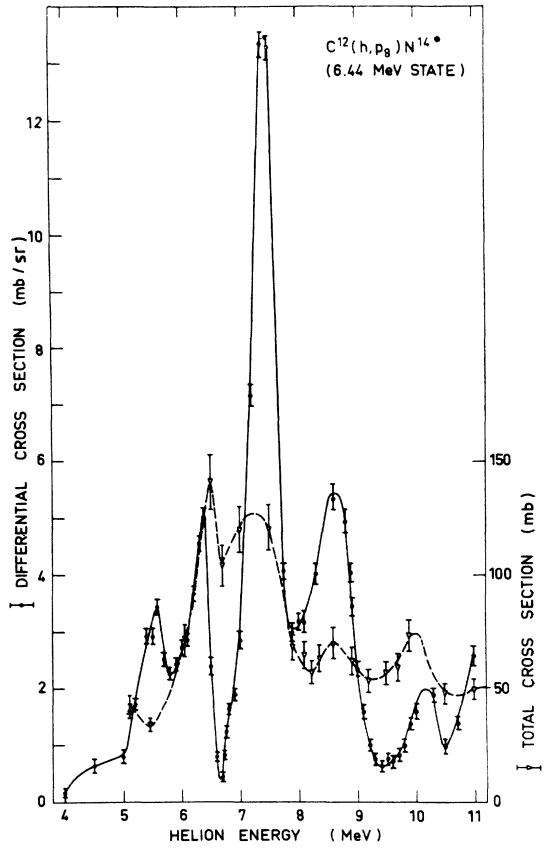

FIG. 4. Differential cross section (solid line and ● points) at a laboratory angle of 172° and total cross section (dashed line and ▽-points) of the proton group from the $C^{12}(h, p_8)N^{14*}$ reaction (6.44-MeV state).

[12] S. Gorodetzky, R. M. Freeman, A. Gallmann, and F. Haas, Phys. Rev. **149**, 801 (1966).

[13] S. Gorodetzky, R. M. Freeman, A. Gallmann, F. Haas, and B. Heusch, Phys. Rev. **155**, 1119 (1967).

obtained at 20.1[6] and 25.3 MeV.[5] In the 20.1-MeV data, unfortunately, the integration has only been carried out for $10° \leq \theta \leq 70°$, but the comparison is nonetheless instructive.

A. 7.03-MeV level: $J^\pi T = 2^+0$; $\psi \simeq 1.00$ $(p_{3/2}, p_{1/2})^{-1}$. Figures 1 and 2 present, respectively, the measured angular distributions, the $\theta_{lab} = 172°$ differential excitation function, and the variation of the total cross section with helion energy for the proton group feeding the 7.03-MeV level.

There is clearly no obvious correlation between the gross behavior of the angular distributions and the

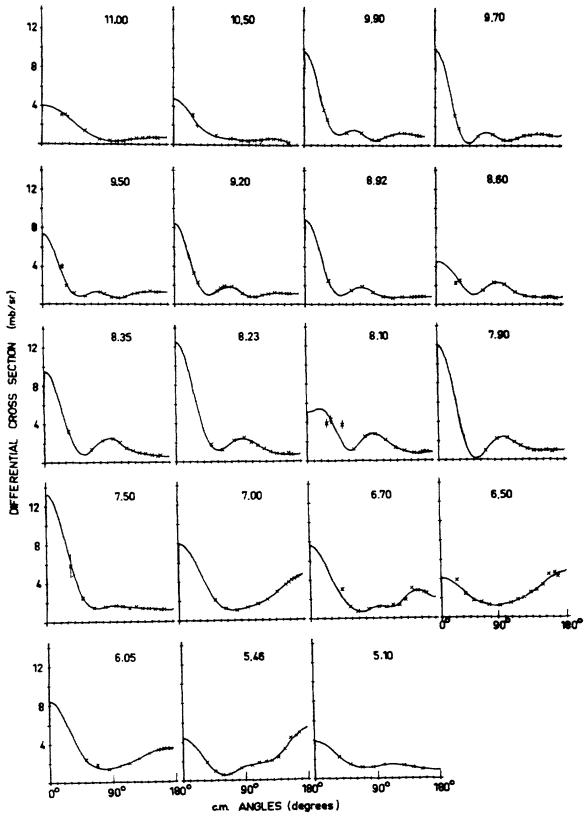

FIG. 5. Proton angular distributions form the $C^{12}(h, p_7)N^{14*}$ reaction (6.21-MeV state) measured in the 5.10–11.0-MeV helion energy range. The solid line is the best fit obtained with a Legendre polynomial expansion via a least-squares calculation.

structure of the total cross-section excitation function. In particular, the well-developed resonance maxima in the latter do not correspond in any unique way to a characteristic distribution shape as was the case in the earlier reported $O^{16}(h, \alpha)O^{15}$ study.

It is clear from Fig. 1, however, that the distribution shapes change systematically with energy over energy intervals of 1–2 MeV as distinct from the now familiar statistical fluctuation phenomena. In gross fashion, the relatively isotropic angular distributions at the lowest energies develop marked forward and/or back-

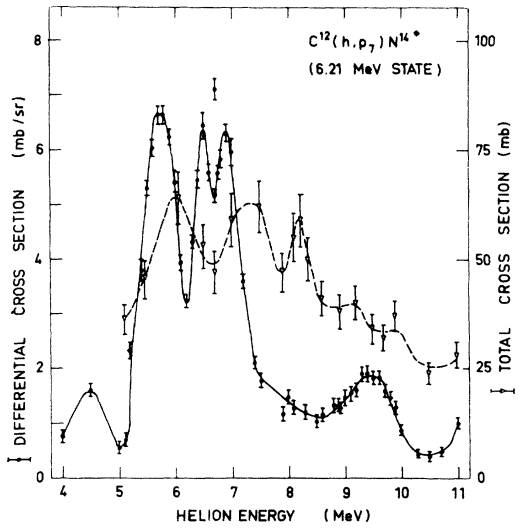

FIG. 6. Differential cross section (solid line and ● points) at a laboratory angle of 172° and total cross section (dashed line and ▽ points) of the proton group from the $C^{12}(h, p_7)N^{14*}$ reaction (6.21-MeV state).

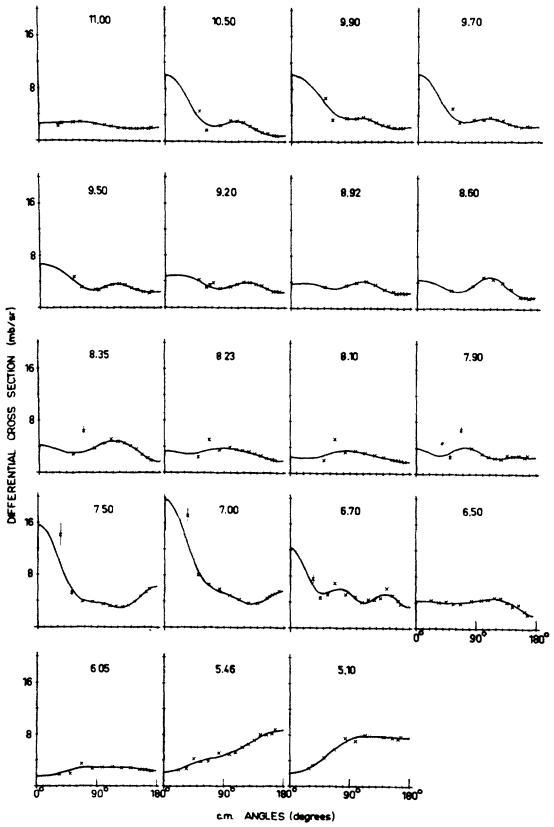

FIG. 7. Proton angular distributions from the $C^{12}(h, p_6)N^{14*}$ reaction (5.83-MeV state) measured in the 5.10–11.0-MeV helion energy range. The solid line is the best fit obtained with a Legendre polynomial expansion via a least-squares calculation.

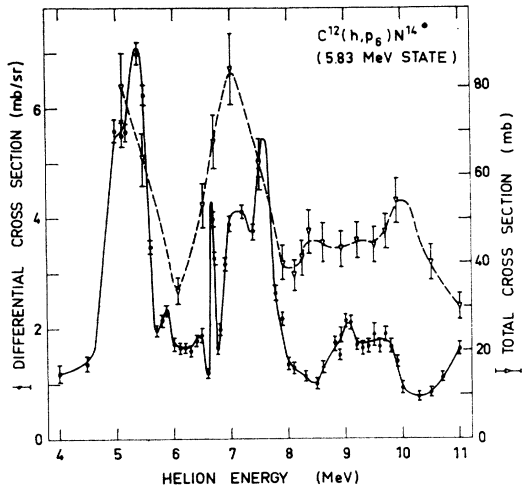

FIG. 8. Differential cross section (solid line and ● points) at a laboratory angle of 172° and total cross section (dashed line and ▽ points) of the proton group of the $C^{12}(h, p_6)N^{14*}$ reaction (5.83-MeV state).

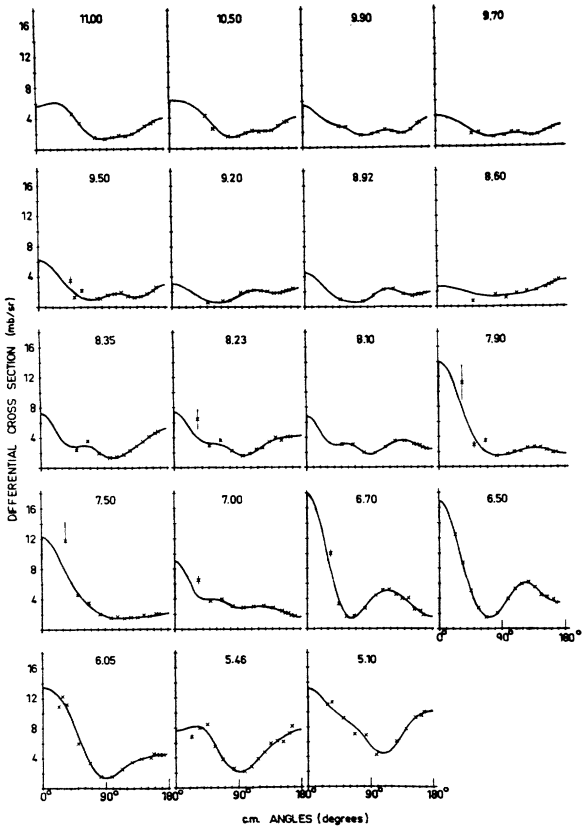

FIG. 9. Proton angular distributions from the $C^{12}(h, p_5)N^{14*}$ reaction (5.69-MeV state) measured in the 5.10–11.0-MeV helion energy range. The solid line is the best fit obtained with a Legendre polynomial expansion via a least-squares calculation.

ward peaking with increasing energy, suggestive of the growing importance of direct reaction amplitudes. The three resonant peaks of the total cross section in Fig. 2 have typically $T\sim1$ MeV. We shall return below to a more detailed examination of these data together with the relevant correlation study input.

B. 6.44-MeV level: $J^\pi T=3^+0$; $\psi=0.81s_{1/2}d_{5/2}+0.44(d_{5/2})^2$. Figures 3 and 4 show the corresponding data for the proton group feeding this level which, in contrast to that at 7.03 MeV, has no hole character and could therefore be populated directly via two nucleon transfer to the ~40% closed $p_{3/2}$ shell component of the C^{12} ground state. As anticipated, the cross section is strikingly higher (see Table I). Beyond the fact that the total cross sections show resonances at $E_h\sim6.5$ MeV, there is no obvious correlation between the cor-

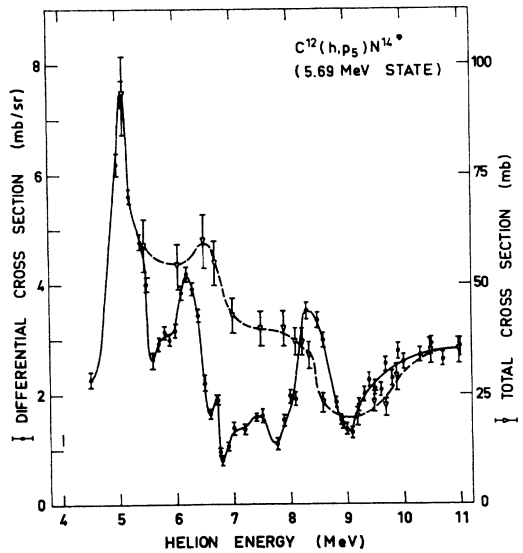

FIG. 10. Differential cross section (solid line and ● points) at a laboratory angle of 172° and total cross section (dashed line and ▽ points) of the proton group from the $C^{12}(h, p_5)N^{14*}$ reaction (5.69-MeV state).

responding data of Figs. 2 and 4; in particular, the resonance at $E_h\sim7.45$ MeV does not appear in Fig. 2. A strong resonance at $E_h=2.99$ has been reported for population of this state; at 2.99 MeV, the angular distribution of protons is isotropic, whereas here at $E_h\sim7.45$ MeV, as evident in Fig. 3, there is a pronounced backward peaking.

C. 6.21-MeV level: $J^\pi T=1^+0$; $\psi=0.83(s_{1/2})^2+0.36(d_{3/2}, d_{5/2})+0.35(d_{5/2})^2$. Figures 5 and 6 show corresponding data for this level. As is clear from Fig. 5, the angular distributions are marked, throughout this energy range, by a dominant forward peaking. This has been observed previously[14] for $2.88\leq E_h\leq4.88$ MeV.

[14] Hsin-Min Kuan, T. W. Bonner, and J. R. Risser, Nucl. Phys. 51, 481 (1964).

D. 5.83-MeV level: $J^\pi T = 3^-0$; $\psi = 0.99(p_{1/2}d_{5/2}) - 0.12(d_{3/2}, f_{7/2})$. Figures 7 and 8 present the data for this negative-parity level. To a striking extent, the angular distributions are relatively isotropic except for forward peaking in the vicnity of $E_h = 7.00$ and 10.0 MeV. There appears to be unusually rapid variation of the backward cross section with energy near 6.7 MeV, although the angular distribution taken at 6.70 MeV fails to show strong peaking.

E. 5.69-MeV level: $J^\pi T = 1^-0$; $\psi = 0.99(p_{1/2}s_{1/2}) + 0.14(p_{1/2}d_{3/2}.)$ Figures 9 and 10 show corresponding data for this level. Including earlier work at $E_h =$

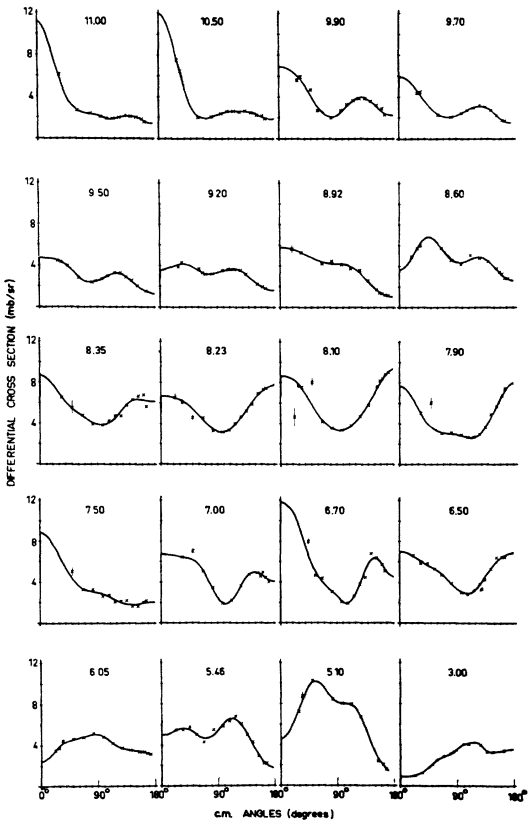

FIG. 11. Proton angular distributions from the $C^{12}(h, p_4)N^{14*}$ reaction (5.10-MeV state) measured in the 3.0–11.0-MeV helion energy range. The solid line is the best fit obtained with a Legendre polynomial expansion via a least-squares calculation.

4.88 MeV, it is clear that the total cross section goes through a strong maximum in the region of 5.0 MeV and decreases rather regularly thereafter. The angular distributions are relatively symmetric relative to 90° except in the vicinity of 6.50 MeV, where forward peaking is pronounced.

F. 5.10-MeV level: $J^\pi T = 2^-0$; $\psi = 0.96(p_{1/2}d_{5/2}) - 0.22(d_{3/2}f_{1/2})$. Figures 11 and 12 show the relevant data. Over all, there appears a tendency toward symmetry relative to 90° in the angular distributions except at the highest energies. The total cross section again

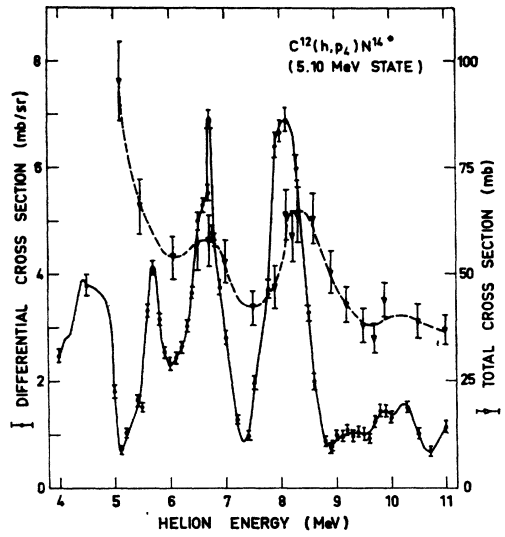

FIG. 12. Differential cross section (solid line and ● points) at a laboratory angle of 172° and total cross section (dashed line and ▽ points) of the proton group from the $C^{12}(h, p_4)N^{14*}$ reaction (5.10-MeV state).

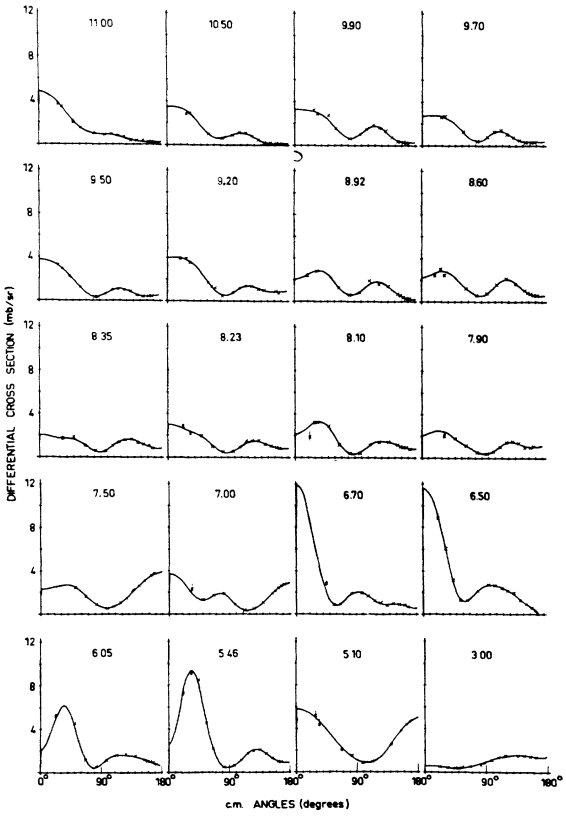

FIG. 13. Proton angular distributions from the $C^{12}(h, p_3)N^{14*}$ reaction (4.91-MeV state) measured in the 3.0–11.0-MeV helion energy range. The solid line is the best fit obtained with a Legendre polynomial expansion via a least-squares calculation.

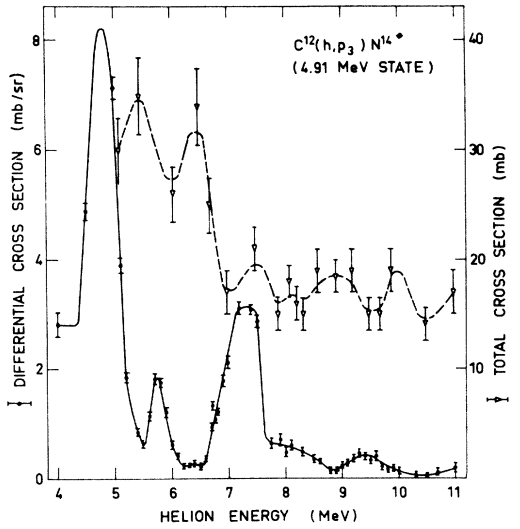

FIG. 14. Differential cross section (solid line and ● points) at a laboratory angle of 172° and total cross section (dashed line and ▽ points) of the proton group from the $C^{12}(h, p_3)N^{14*}$ reactio (4.91-MeV state).

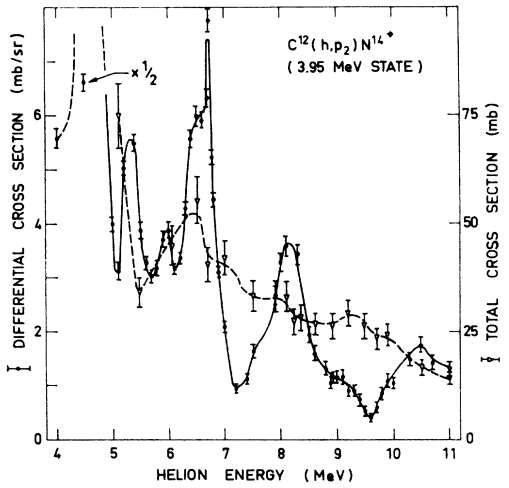

FIG. 16. Differential cross section (solid line and ● points) at a laboratory angle of 172° and total cross section (dashed line and ▽ points) of the proton group from the $C^{12}(h, p_2)N^{14*}$ reaction (3.95-MeV state).

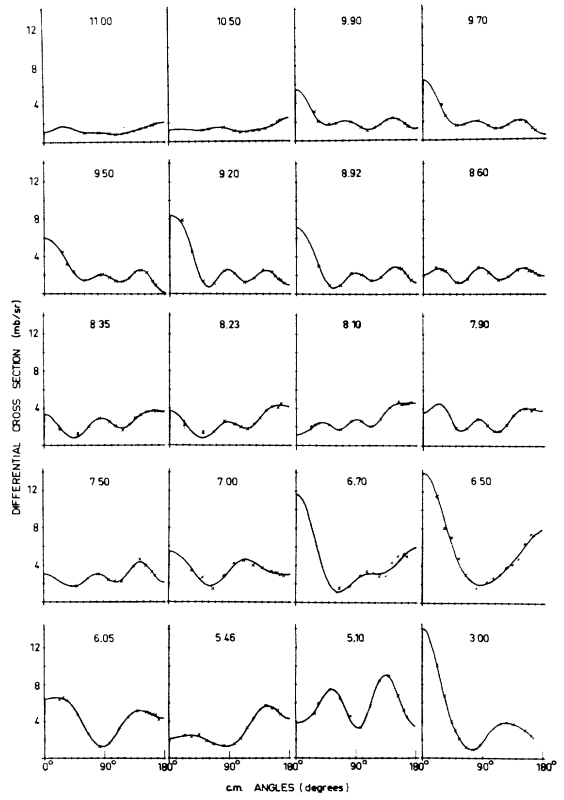

FIG. 15. Proton angular distributions from the $C^{12}(h, p_2)N^{14*}$ reaction (3.95-MeV state) measured in the 3.0–11.0-MeV helion energy range. The solid line is the best fit obtained with a Legendre polynomial expansion via a least-squares calculation.

shows a strong peaking at $E_h \sim 5$ MeV if earlier work[14] at 4.88 MeV is included.

G. 4.91-MeV level: $J^\pi T = 0^- 0$; $\psi = 1.00(p_{1/2}s_{1/2})$. Figures 13 and 14 present the data for this level. The angular distributions show no strong forward or backward peaking, except for the region of $E_h \sim 6.5$ MeV

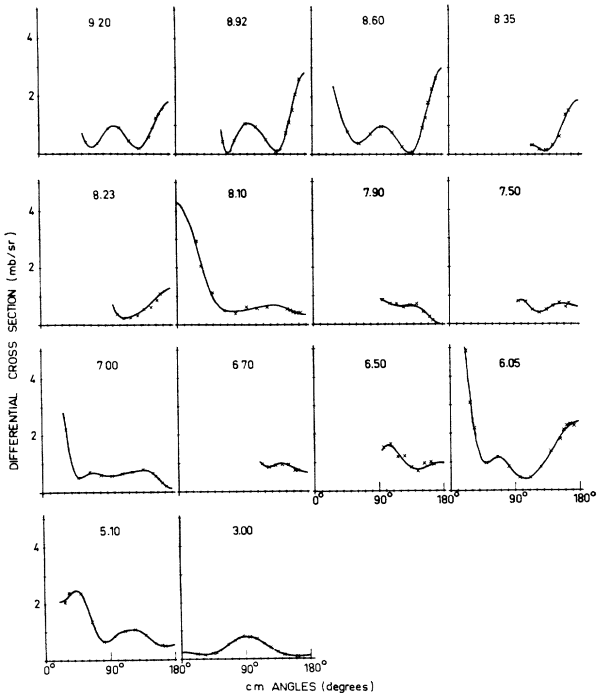

FIG. 17. Proton partial angular distributions from the $C^{12}(h, p_1)N^{14*}$ reaction (2.31-MeV state) measured in the 3.0–9.2-MeV helion energy range. The solid line is the best fit obtained with a Legendre polynomial expansion via a least-squares calculation.

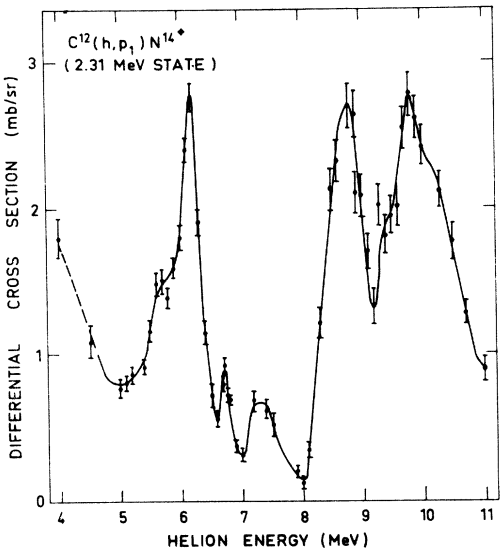

FIG. 18. Differential cross section at a laboratory angle of 172° for the proton group from the $C^{12}(h, p_1)N^{14*}$ reaction (2.31-MeV state).

where the distributions and energy behavior are remarkably similar to those shown in Fig. 9 for the 1^-0, 5.69-MeV level.

H. 3.95-MeV level: $J^\pi T = 1^+0$; $\psi = 0.93(p_{3/2}p_{1/2})^{-1} - 0.32(p_{3/2})^2$. Figures 15 and 16 are appropriate to this level. Again the angular distributions undergo rapid change near $E_h = 6.5$ MeV and the total cross section decreases rather smoothly with increasing energy. We shall comment below on the fact that the total cross-section data of Fig. 16 are so different from those of Fig. 2, even though the two residual states have very similar configurations as members of the dominant $(p_{3/2}, p_{1/2})^{-1}$ quartet of states. As before, if we include earlier results, the total cross section for population of this level peaks between 4 and 5 MeV of incident energy.

I. 2.31-MeV level: $J^\pi T = 0^+1$; $\psi = 0.91(p_{1/2})^2 - 0.40(p_{3/2})^{-2}$. Figure 17 presents partial proton angular distributions and Fig. 18 the $\theta_{lab} = 172°$ differential

TABLE II. Multipole amplitude ratios for the 7.03-MeV transition in N^{14}.

Author	$\delta = \langle \| E2 \| \rangle / \langle \| M1 \| \rangle$
Gorodetzky *et al.*[a]	$+(0.60\pm0.20)$
Gallmann *et al.*[b]	$+(0.70\pm0.10)$
Swann[c]	$+(0.60\pm0.15)$
Prosser *et al.*[d]	$+(0.60\pm0.10)$
Weighted average	$+(0.637\pm0.028)$

[a] Reference 13.
[b] Reference 9.
[c] Phys. Rev. **148**, 1119 (1966).
[d] Phys. Rev. **129**, 1716 (1963).

TABLE III. Legendre polynomial coefficients for the angular correlation of the 7.03-MeV N^{14} state deexcitation.

Incident helion energy (MeV)	a_2/a_0	a_4/a_0
4.62	-1.05 ± 0.06	$+0.14\pm0.08$
4.90	-0.97 ± 0.06	$+0.06\pm0.05$
5.11	-1.04 ± 0.07	$+0.18\pm0.07$
	-1.02 ± 0.03	$+0.21\pm0.04$
5.46	-1.05 ± 0.11	$+0.25\pm0.12$
6.05	-0.82 ± 0.04	$+0.07\pm0.03$
6.50	-0.90 ± 0.03	$+0.11\pm0.03$
6.70	-0.85 ± 0.03	$+0.08\pm0.02$
7.0	-0.63 ± 0.08	-0.06 ± 0.07
7.4	-0.81 ± 0.04	$+0.02\pm0.03$
7.5	-0.81 ± 0.04	$+0.05\pm0.04$
7.7	-0.88 ± 0.04	$+0.09\pm0.03$
8.0	-0.63 ± 0.03	-0.14 ± 0.03
8.5	-0.57 ± 0.03	-0.23 ± 0.02
8.92	-0.66 ± 0.03	-0.20 ± 0.02
9.5	-0.72 ± 0.04	-0.09 ± 0.04
9.60	-0.79 ± 0.03	-0.01 ± 0.02
9.80	-1.00 ± 0.03	$+0.24\pm0.02$
10.0	-1.03 ± 0.04	$+0.25\pm0.03$
10.2	-1.02 ± 0.03	$+0.26\pm0.02$
10.4	-0.77 ± 0.03	$+0.01\pm0.02$
10.5	-0.72 ± 0.02	-0.07 ± 0.02
11.0	-0.52 ± 0.06	-0.20 ± 0.05

TABLE IV. Populations $P(0)$, $P(1)$, and $P(2)$ as functions of the incident helion energy.

E_h in MeV	$P(0)$	$P(1)$	$P(2)$
4.62	0.68 ± 0.07	0.16 ± 0.05	0.0 ± 0.06
4.90	0.53 ± 0.09	0.24 ± 0.06	-0.01 ± 0.07
5.11	0.80 ± 0.07	0.08 ± 0.05	0.02 ± 0.06
5.46	0.87 ± 0.11	0.04 ± 0.07	0.03 ± 0.09
6.05	0.51 ± 0.05	0.22 ± 0.03	0.03 ± 0.04
6.50	0.60 ± 0.04	0.18 ± 0.025	0.02 ± 0.03
6.70	0.535 ± 0.035	0.21 ± 0.02	0.025 ± 0.03
7.0	0.335 ± 0.09	0.29 ± 0.06	0.04 ± 0.07
7.4	0.42 ± 0.05	0.27 ± 0.03	0.02 ± 0.04
7.5	0.47 ± 0.07	0.24 ± 0.05	0.025 ± 0.06
7.7	0.56 ± 0.05	0.20 ± 0.03	0.02 ± 0.04
8.0	0.105 ± 0.05	0.43 ± 0.035	0.015 ± 0.04
8.5	-0.06 ± 0.04	0.53 ± 0.03	0.00 ± 0.03
8.92	0.01 ± 0.04	0.505 ± 0.03	-0.01 ± 0.03
9.5	0.11 ± 0.07	0.39 ± 0.05	0.01 ± 0.06
9.6	0.37 ± 0.035	0.30 ± 0.02	0.03 ± 0.04
9.8	0.84 ± 0.04	0.04 ± 0.03	0.03 ± 0.04
10.0	0.87 ± 0.06	0.035 ± 0.04	0.03 ± 0.05
10.2	0.88 ± 0.045	0.02 ± 0.03	0.04 ± 0.04
10.4	0.40 ± 0.035	0.28 ± 0.02	0.02 ± 0.03
10.5	0.25 ± 0.035	0.36 ± 0.02	0.01 ± 0.03
11.0	-0.03 ± 0.07	0.49 ± 0.05	0.02 ± 0.06

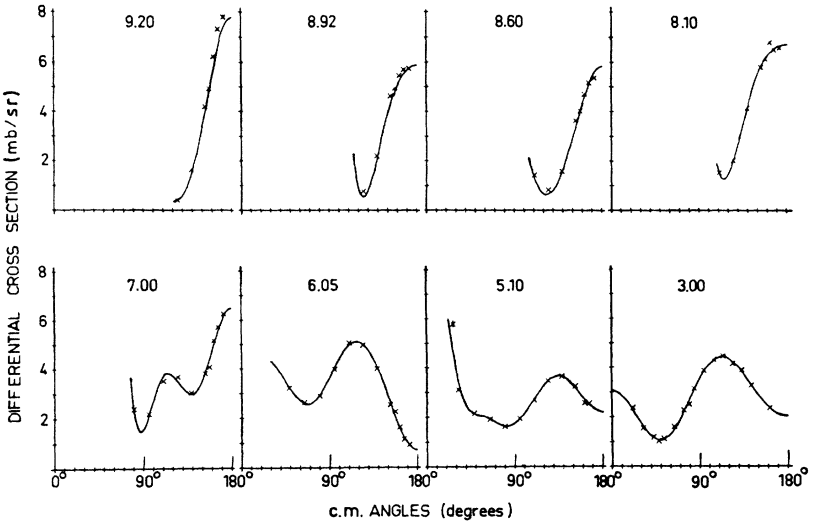

FIG. 19. Proton group partial angular distribution from the $C^{12}(h, p_0)N^{14}$ reaction (ground state) measured in the 3.0–9.2-MeV helion energy range. The solid line is the best fit obtained with a Legendre polynomial expansion via a least-squares calculation.

excitation function corresponding to this state. Inasmuch as it was experimentally inconvenient to obtain complete angular distributions here, we do not give the total cross section variation with energy; it is not immediately relevant to our considerations in any case.

J. Ground state: $J^\pi T = 1^+0$; $\psi = 0.98(p_{1/2})^2 - 0.21(p_{3/2}, p_{1/2})^{-1}$. Figures 19 and 20 present selected angular distributions and partial information on the excitation function for the proton group populating the ground state. At higher energies in our range, a pronounced backward peak is evident.

Figure 21 is a synthesis of all the total excitation-function data from the present measurements. From this figure it is evident that there is significant structure in the excitation functions, and the correlations between different channels would suggest the presence of resonances at the following approximate helion energies: 4.5, 5.5, 6.4, 7.4, 8.2, 8.6, and 10 MeV.

Those at 10, at 6.4, and at 4.5 MeV appear in the greatest number of reaction channels. There are no obvious correlations between participation of a resonance in a given channel and the spin or parity of the residual state involved in the reaction channel.

TABLE V. Legendre polynomial coefficients for the angular correlations of the 5.10-, 5.69-, 5.83-, 6.21-, and 6.44-MeV N^{14} state deexcitations at 8.5-MeV helion energy.

Excitation energy (MeV)	Transition energy (MeV)	a_2/a_0	a_4/a_0
5.10	2.79	+0.53±0.07	−0.62±0.09
	5.10	+0.05±0.03	−0.23±0.03
5.69	3.38	−0.29±0.05	
	5.69	+0.22±0.04	
5.83	2.79	+0.46±0.21	−0.18±0.23
	5.83	+0.84±0.12	+0.10±0.12
6.21	3.90	−0.61±0.04	
	6.21	+0.06±0.07	
6.44	6.44	+0.54±0.03	−0.37±0.03

IV. ANGULAR CORRELATION DATA

A. 7.03-MeV level. As indicated above, we have concentrated upon study of the proton-γ angular correlation involving the 2^+, $T=0$, 7.03-MeV state because of our discovery of rapid variation with energy between essentially pure $m=0$ and $|m|=1$ substate population. This earlier work was carried out at $E_h=5.11$ and 8.92 MeV; we now report on a systematic study of this phenomenon for $4.5 \leq E_h \leq 11.0$ MeV.

In the interest of efficiency, recognizing that many angular correlations were required, and knowing the

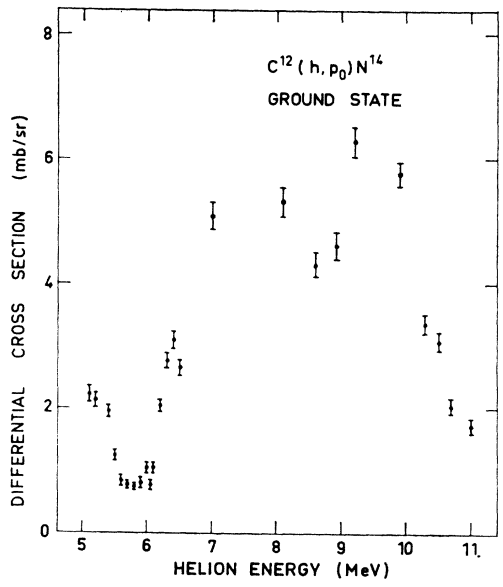

FIG. 20. Differential cross section at a laboratory angle of 172° for the proton group from the $C^{12}(h, p_0)N^{14}$ reaction (ground state).

TABLE VI. Legendre polynomial coefficients a_2/a_0 and populations $P(0)$ and $P(1)$ as functions of the incident energy relative to the 6.21- and 5.69-MeV N^{14} states.

Excitation energy (MeV)	E_h (MeV)	a_2/a_0	$P(0)$	$P(1)$
6.21	4.62[a]	−0.14±0.06	0.43±0.04	0.285±0.02
	4.90[a]	−0.89±0.05	0.94±0.04	0.03±0.005
	5.11[a]	−0.34±0.09	0.57±0.06	0.215±0.035
	5.46[a]	−0.28±0.04	0.52±0.04	0.24±0.02
	8.50	−0.61±0.04	0.75±0.03	0.12±0.015
	8.92[b]	−0.05±0.05	0.37±0.04	0.32±0.04
5.69	4.62[a]	−0.39±0.10	0.60±0.07	0.20±0.03
	4.90[a]	−0.27±0.10	0.52±0.07	0.24±0.03
	5.46[a]	−0.14±0.06	0.43±0.04	0.285±0.02
	8.50	−0.29±0.05	0.54±0.04	0.23±0.02
	8.92[b]	−0.18±0.07	0.46±0.06	0.27±0.025

[a] Results reported in Ref. 12.

[b] Results reported in Ref. 9.

amplitude ratio in the ground-state deexcitation transition, only three angles were used (0°, 45°, and 90°) in each individual correlation. In effect, the determination of the correlation function W (45°) relative to W (0°) and W (90°) sufficies to define the a_4 coefficient when, as in this case, the multipole amplitude ratio in the transition is known.

The measured correlation data were fitted to the usual Legendre polynomial expansion, namely,

$$W(\theta)=\sum_k \rho_k(2)F_k(2,1)Q_kP_k(\cos\theta)$$
$$=\sum_k a_kP_k(\cos\theta), \qquad k=0, 2, 4.$$

The values of the multipole amplitude ratio for the ground-state deexcitation transition from the 7.03-MeV state has been measured previously as noted in Table II. Having given this, the theoretical correlation function $W(\theta)$ is a function only of the population parameters $P(0)$ and $P(1)$ and— to the extent permitted by the finite backward counter solid angle— $P(2)$. We have included this possibility in fitting the experimental data subject to the obvious normalization condition that $P(0)+2P(1)+2P(2)=1$. For our geometry, the attenuation coefficients Q_k have the values 0.97 and 0.91, for $k=2$ and 4, respectively. The Legendre polynomial coefficient ratios may be expressed as

$$a_2/a_0=-1.2278[2P(0)+3P(1)-1],$$
$$a_4/a_0=+0.1001[\tfrac{5}{2}P(0)-5P(1)+\tfrac{1}{2}].$$

Table III lists the coefficient ratios obtained at the 22 different helion energies examined in the range $4.62\leq E_h\leq 11$ MeV, while Table IV lists the corresponding population parameters for the three substates. As is evident from this Table, $P(2)$ never attains a value in excess of 5%, which is consistent with the empirical estimating expressions which have been published previously.

Figure 22 shows the values of $P(0)$ obtained as functions of the incident helion energy. Structure in this curve corresponds to the above mentioned resonances at 5.5, 6.4, 7.4, and 10.0 MeV. Although more complete measurements would be required to establish the presence or absence of structure at the 8.2- and 8.6-MeV resonances, the present data do appear to preclude any strong resonant behavior at these energies. Figure 23 shows the partial differential cross section $\sigma(0)=P(0)(d\sigma/d\Omega)\theta_{\rm lab}=172°$ and $\sigma(1)=P(1)(d\sigma/d\Omega)\theta_{\rm lab}=172°$, together with the total cross section for population of the 7.03-MeV state. Both partial cross sections

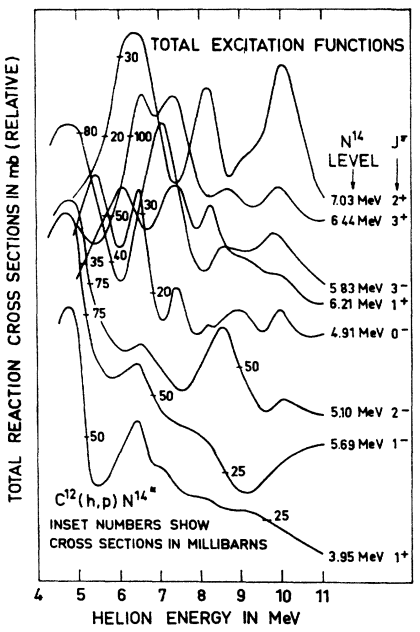

FIG. 21. Synthesis of all the excitation-function data measured at a laboratory angle of 172° corresponding to the proton groups leading to population of the indicated 10 bound levels of N^{14} in the $C^{12}(h, p)N^{14}$ reaction.

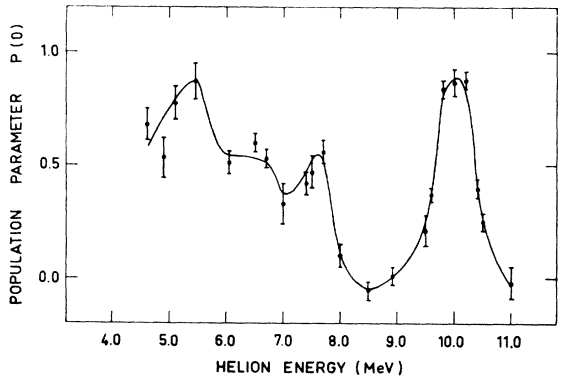

FIG. 22. Values, for the 7.03-MeV state population parameter $P(0)$, of the $m=0$ magnetic substate, plotted as a function of the incident helion energy in the range 4.62–11.0 MeV.

resonate at the 6.4-MeV resonance, whereas only $\sigma(0)$ resonates at the 10-MeV resonance. Only $\sigma(1)$ resonates strongly at 8.2 and 8.6 MeV where $\sigma(0)\approx 0$; $\sigma(0)$ also resonates at $\sim$7.8 MeV. We shall return to a discussion of these phenomena below.

B. 6.44- and 5.10-MeV levels. As was noted previously, the available instrumentation did not permit simultaneous study of the correlation for all states of interest in N^{14}. Of particular interest, for reasons already given, are those states for which the strong deexcitation transitions have well known multipole amplitudes ratios *or* for which these transitions proceed to the 0^+ state at 2.31 MeV in which case they are necessarily of pure multipole character. (The states at 3.95, 5.69, and 6.21 MeV particularly satisfy this last criterion having deexcitation branches of 96, 64, and 79%, respectively, to the 2.31-MeV state.) The case of the 3.95-MeV state is of particular interest inasmuch as it and the 7.03-MeV state, which we have studied in detail, are the two upper members of the $(p_{3/2}, p_{1/2})^{-1}$ quadruplet in N^{14}. Fragmentary measurements have been reported on the deexcitation of the 5.10-MeV state populated in the $C^{12}(h, p)N^{14}$ reaction[15]; at 3.1- and at 4.9-MeV helion energies, respectively, it is reported that $P(0)\simeq(40+15\%)$ and $>86\%$, respectively.

We have carried out isolated correlation measurements at $E_h=8.5$ MeV and in Table V we list the Legendre polynomial coefficient ratios for five selected N^{14} states. In these measurements, we have taken data at two additional angles, namely, 30° and 60°. In considering these data, together with those given in Table I of Ref. 12 and in Table I of Ref. 9, it is immediately clear that we do not find effects as striking as in the case of the 7.03-MeV level; however, there remain substantial variations with energy. In Table VI, we list the results of a analyses on the 3.90- and 3.38-MeV transitions from the indicated states to that at 2.31 MeV. In these cases, for $J=1\rightarrow J=0$ transitions,

$$a_2/a_0=-0.9700[P(0)-P(1)]$$

and

$$P(0)+2P(1)=1.$$

It is interesting to note that we have found no positive value for a_2/a_0 in Table VI; complete alignment of the states in the $|m|=1$ magnetic substate would require that $a_2/a_0=+0.48$. This is simply a further indication that the alignment here is much less complete than in the case of the 7.03-MeV state.

V. DISCUSSION OF RESULTS

As is obvious in the foregoing presentation of results, no single simple reaction mechanism can suffice to explain the observed phenomena in this energy range; while the excitation functions show pronounced resonance phenomena, in some channels, the systematic development of characteristic angular distribution features such as forward and backward peaking, even in these same channels, suggests the importance of direct reaction amplitudes.

Glendenning[16] has considered the latter mechanism in some detail and has developed a microscopic mechanism theory which permits calculation of the anticipated angular and energy dependence of the cross section on the assumption of specific model wave functions for the states in question and distorting optical-model potentials in the entrance and exit channels. In view of the obvious importance of compound-system effects in the present data, we have not considered it worthwhile to engage in such distorted-wave Born-approximation (DWBA) studies, although they have been quite suc-

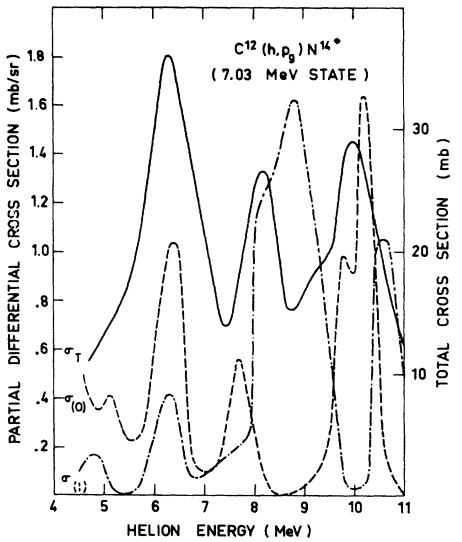

FIG. 23. Partial differential cross sections $\sigma(0)$ and $\sigma(1)$ and total cross sections for the 7.03-MeV state. Definition of $\sigma(0)$ and $\sigma(1)$ is given in the text.

[15] R. S. Blake, D. J. Jacobs, J. O. Newton, and J. P. Schapira, Phys. Letters **14**, 219 (1965).

[16] N. K. Glendenning, Phys. Rev. **137**, B102 (1965).

cessful in correlation data obtained at the higher helion energies.

Of importance, however, are the selection rules for the (h, p) reaction as discussed by Glendenning. In the present case of a $J=0$, $T=0$ target, it is clear that the J_f, T_f of the residual N^{14} state must be identical to the J, T of the transferred nucleons (assuming for the immediate discussion, a two-nucleon transfer mechanism). Recognizing that the nucleons are in relative s states in the helion, it follows that if $T_f=1$, then $J_f=L$, where $\mathbf{J}=\mathbf{L}+\mathbf{S}$, and all $T_f=1$, then unnatural-parity final states are forbidden in the reaction. If $T_f=0$, similarly, $S=1$ and $J_f+1\geq L\geq |J_f-1|$ with $\pi_f=(-1)^L$. The important consequence is that these selection rules allow only a single value of L, the transferred orbital angular momentum, to contribute to the population of natural-parity final states, whereas two values are permitted in the case of unnatural-parity final states. In the higher-energy studies,[5,6] these rules have been tested successfully.

In the present work, the fact that the excitation functions for the 7.03- and 3.95-MeV states—the two upper members of the $(p_{3/2}, p_{1/2})^{-1}$ quadruplet in N^{14}—have strikingly different structure, despite very similar wave functions for the final states involved, may reflect this latter rule. In the case of the 7.03-MeV level, only $L=2$ is permitted, whereas both $L=0$ and $L=2$ can contribute to the population of the 3.95-MeV level with consequent smearing out of overlapping resonant phenomena. No such general remarks may be made concerning the remaining data of Fig. 21, for example, without the availability of a detailed reaction-mechanism model which takes specific cognizance of the residual state wave functions.

7.03-MeV Level. To the extent that C^{12} was a pure j-j coupling nucleus, i.e., with a closed $p_{3/2}$ subshell, direct two-nucleon transfer to the 2^+ 7.03-MeV state would be completely forbidden in view of its $(p_{3/2}, p_{1/2})^{-1}$ wave function. There is strong evidence, however, that such a pure $(j-j)$ picture is unrealistic; Cohen and Kurath[8] have calculated a model wave function

$$\psi(C^{12})=0.612(p_{1/2})^0+0.261(p_{1/2})_A{}^2+0.625(p_{1/2})_B{}^2 +0.255(p_{1/2})^3+0.319(p_{1/2})^4$$

assuming only a closed He^4 core. Detailed comparison with the total cross-section data at 20.1 MeV has demonstrated that the wave functions of the Cohen-Kurath model[8] for N^{14} are much preferable to those of the True model[7] which assumes a closed $(p_{3/2})C^{12}$ core, except in the case of N^{14} states having a dominant (s, d) configuration.

As noted above, the $(p_{1/2})^0$ term in the C^{12} wave function cannot contribute to the direct two-nucleon population of the 7.03-MeV state; similarly, the $(p_{1/2})^4$ term is excluded. In the case of the $(p_{1/2})_{A/B}{}^2$ terms, one of the transferred nucleons would necessarily strip into a $p_{1/2}$ and the other into a $p_{3/2}$ orbit; to the extent that the two-nucleon direct transfer reactions are characterized by transfer of a closely spatially correlated nucleon pair, this would require $S=0$ which is not allowed for $T_f=0$. Failing spin-flip then, these terms also do not contribute. In consequence, only the $(p_{1/2})^3$ term comprising some 6% of the C^{12} ground state can be involved in direct non-spin-flip two-nucleon transfer population of the 7.03-MeV state. The fact that the total cross section, apart from the case of the 6.44-MeV state noted above, is roughly comparable for the 7.03-MeV state and for the remaining low states in N^{14} again suggests important compound-system contributions. In order to examine this suggestion further, we have examined the Legendre polynomial coefficient ratios a_k/a_0 as functions of the incident helion energy in the range studied. The results are shown in Fig. 24 for the angular distributions of protons leading to population of the 7.03-MeV state. Of greatest interest is the fact that for $k=6$ and above, the ratios are essentially zero, implying vanishing contributions for higher partial waves in the incident beam. This behavior is strongly supportive of a compound-system mechanism.

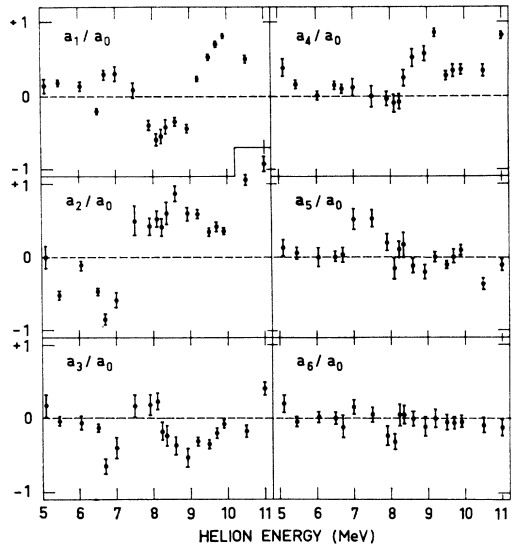

FIG. 24. Variation with bombarding energy of the expansion coefficients a_k/a_0 for the $C^{12}(h, p_9)N^{14}$ (7.03-MeV state) angular distributions.

As indicated in Table I, in particular, the average total-cross section to the 7.03-MeV level is roughly half that to the 3.95-MeV state. For given (L, S), the cross sections should be proportional to

$$R=(2J_f+1)N(N+1)\langle \mathrm{CFP}\rangle^2,$$

where J_f is the total angular momentum of the final state, N is the number of active nucleons (10 p shell nucleons in the case of N^{14}), and the $\langle \mathrm{CFP}\rangle$ are the appropriate two-particle coefficients of fractional parentage.

$$\langle J_f T_f \alpha(A=14)\,||\,00\mathrm{g.s.}(C^{12}); JT, LS\rangle,$$

which have been calculated by Kurath. In the case of the 7.03-MeV state, only $(L, S)=(2, 1)$ and $(0,1)$ are allowed, and $R=0.004$ and 2.06, respectively; for the ground state, for comparison, $R=2.13$ and 0.085, respectively. In the j-j limit, only the ground state would be significantly populated, and inasmuch as all three states are populated equally to within a factor ~ 2, this provides additional evidence against the j-j limit for C^{12}.

As noted above, there are three relatively pronounced resonances in the total excitation function for the 7.03-MeV level at 6.4-, 8.2-, and 10.0-MeV helion energy. These resonances have characteristic widths ~ 1 MeV. These, together with the above discussion, suggest consideration of the compound-system phenomena which must produce such structure. At the same time, any such explanation must include the behavior of the partial cross sections $\sigma(1)$ and $\sigma(0)$ as shown in Fig. 23.

In general, we may write that the cross section will be proportional to the product of an entrance and an exit channel overlap integral of the form

$$|\langle C^{12}+h \mid \psi_J\rangle|^2 \,|\langle \psi_J \mid N^{14*}+p\rangle|^2,$$

where ψ_J is the compound state of spin J involved. We focus attention on the exit channel to consider under what conditions population of only $|m|=1$ or $m=0$ substates of the final N^{14*} state might be anticipated and in particular, we focus on the 2^+, 0, 7.03-MeV state for which we have data as shown in Fig. 23.

We assume that we may write ψ_J as follows:

$$\psi_J=\sum_\nu \alpha_\nu\{J_f{}^\pi T_f; l_j\}_J+\sum_\mu \beta_\mu\Phi_\mu,$$

where l_j represents the available single-particle orbitals in this mass region which could couple to an effective N^{14} excited core in the $J_f{}^\pi T_f$ configuration to yield the compound system J, and Φ_μ are the remaining terms required for a complete specification of ψ_J. In particular, however, the Φ_μ are orthogonal to the particle-core coupled terms of the first summation. Provided that we restrict l_j to represent only $s_{1/2}$, $d_{5/2}$, and $d_{3/2}$ orbitals, as appears reasonable at least for the present discussion purposes, we may ignore antisymmetrization problems since $\psi(7.03\text{ MeV})^8$ is $1.00)p_{3/2}, p_{1/2})^{-1}$. In particular, Φ_μ will include the reaction entrance channel such that at the time of formation one or more of the β_μ will be nonzero subject only to the condition that $\sum_\mu|\beta_\mu{}^2+\sum_\nu|\alpha_\nu|^2=1$. The residual interaction will then bring about a relaxation population of the remaining β_μ and α_ν to their equilibrium values characteristic of ψ_J in a time short compared to the intrinsic lifetime of the compound state.

With a quantization axis defined by the beam and proton detection directions (0^0 and $\sim 180°$, respectively), it follows that only $|m|=\frac{1}{2}$ substates of ψ_J are populated in the entrance channel; the Litherland and Ferguson method-II geometry used in the correlation studies implies that the outgoing proton can carry a z component of total angular momentum m_p of $\pm\frac{1}{2}$ with the consequence that only the $|m|=1$ and 0 substates of the residual nucleus are accessible. Without loss of generality, we may consider only the $m_J=+\frac{1}{2}$ substate of ψ_J; it follows that $m=1$ is correlated with $m_p=-\frac{1}{2}$ and $m=0$ is correlated with $m_p=+\frac{1}{2}$. The quantities of interest then are the overlap integrals

$$P_m=|\langle\psi_{J,1/2}\mid\Phi_{N^{14}}(J_fT_f, m)\chi_p(l_p, m_{l_p}, m_p)\rangle|^2.$$

In these overlap integrals, only the first summation in the expression for ψ_J enters and we find P_m given by

$$P_m\sim|\sum_{\nu l_p}\alpha_\nu C(J_f, j, J; m, \tfrac{1}{2}-m, \tfrac{1}{2})C(l_p, s_p, j; m_{l_p}, \tfrac{1}{2}-m_{l_p}-m, \tfrac{1}{2}-m)|^2,$$

where $s_p=\frac{1}{2}$ and the remaining variables are defined as above.

For initial simplicity in considering the 7.03-MeV data, we include only the possibility of $d_{3/2}$ and $d_{5/2}$ single-proton orbitals and assume $J=\frac{3}{2}$. Under these assumptions,

$$P_0\sim|\alpha_1C(2,\tfrac{3}{2},\tfrac{3}{2};0,\tfrac{1}{2},\tfrac{1}{2})C(2,\tfrac{1}{2},\tfrac{3}{2};0,\tfrac{1}{2},\tfrac{1}{2})+\alpha_2C(2,\tfrac{5}{2},\tfrac{3}{2};0,\tfrac{1}{2},\tfrac{1}{2})C(2,\tfrac{1}{2},\tfrac{5}{2};0,\tfrac{1}{2},\tfrac{1}{2})|^2,$$

$$P_1\sim|\alpha_1C(2,\tfrac{3}{2},\tfrac{3}{2};1,-\tfrac{1}{2},\tfrac{1}{2})C(2,\tfrac{1}{2},\tfrac{3}{2};0,-\tfrac{1}{2},\tfrac{1}{2})+\alpha_2C(2,\tfrac{5}{2},\tfrac{3}{2};1,-\tfrac{1}{2},\tfrac{1}{2})C(2,\tfrac{1}{2},\tfrac{5}{2};0,-\tfrac{1}{2},\tfrac{1}{2})|^2,$$

and on substitution

$$P_0\sim|0.284\alpha_1+0.185\alpha_2|^2,$$

$$P_1\sim|0.379\alpha_2|^2.$$

In this simple case pure $|m|=1$ population would result in the requirement that $\alpha_1=-0.653\alpha_2$ and pure $m=0$ population would require $\alpha_2=0$. If we include $s_{1/2}$ terms as well, corresponding to $\nu=3$, we find

$$P_0\sim|0.28\alpha_1+0.185\alpha_2+0.632\alpha_3|^2,$$

$$P_1\sim|0.379\alpha_2+0.775\alpha_3|^2,$$

and it is clear that appropriate choice of the α_ν at any given energy—hence compound-system excitation—can result in pure $|m|=1$ or 0 population of the residual state. These arguments are clearly not restricted to $J=\frac{3}{2}$; however, it is instructive to continue this as an illustrative value. At the excitation energies in O^{15} involved here, it may be estimated readily from current level-density formulas[17] that there should be some 30—50 $J=\frac{3}{2}$ levels per MeV. The fact that the partial cross sections shown in Fig. 23 show char-

[17] A. Gilbert, F. S. Chen, and A. G. W. Cameron, Can. J. Phys. **43**, 1248 (1965).

acteristic resonance widths ~0.5–1.0 MeV suggests that we may be dealing with quasigiant resonance phenomena, where a relatively simple particle-excited core configuration such as that described above is dissolved, over regions of this order in energy, into the underlying continuum of more normal compound-system levels. These resonance also suggest that particular phase and magnitude relations in this resonance wave function are reflected in systematic variation of the magnetic substate population of the residual nuclear state, which is identical with the excited core of the resonance.

The situation is particularly simple in the case of the 7.03-MeV state since, as noted above, we can ignore symmetrization effects. This would not be the case if the state contained any s or d orbital components in its wave function. This may explain why the effect is particularly marked in this case.

It will clearly be of interest to examine the correlation data involving the 3.95-MeV level to search for similar effects. The relevant measurements are in progress in this laboratory.

It is interesting to note that this possible occurrence of nuclear states at high excitations having strong particle-plus-excited-core configurations of remarkable simplicity parallels the recent clear discovery of such behavior in the region of lead.[18]

There remains the question of apparent correlation between population of $|m|=1$ substates in the correlation work and the appearance of pronounced backward maxima in the angular distributions. This does not follow in any obvious way from the above considerations and is pronounced in Figs. 2 and 22.

An extremely simple and mechanical view of the reaction mechanism may provide some insight here, but should clearly not be viewed seriously. On the basis of any kinematic argument involving conservation of linear momentum, the presence of a pronounced backward peak suggests heavy-particle stripping wherein the helion would be capture by the target C^{12} and the emergent proton would be derived from the target rather than the projectile. If we assume that C^{12} has a pronounced oblate deformation, as available evidence suggests, the maximum probability for inducing a heavy-particle stripping interaction would result for helions incident on the symmetry axis of the oblate spheroid. Under these conditions, the protons most probably left behind from the target nucleus, as it moved forward under the helion impact, would be those most probably evident in the equatorial zone of the spheroid.

On this basis of simple Nilsson-model arguments for C^{12}, these protons would be those having $\Omega=\frac{3}{2}$, that is a projection of their total angular momentum of $\pm\frac{3}{2}$ along the symmetry axis of the spheroid, hence incident helion direction, in this model. Since the helions carry only $\pm\frac{1}{2}$ as their total angular momentum projections along this same axis, this trivial model automatically correlates the population of only $|m|=1$ substates in the residual nucleus with the occurrence of heavy-particle stripping, and hence backward peaking in the angular distribution.

VI. CONCLUSION

Detailed studies on particle angular distributions and on particle–γ-radiation angular correlations in the $C^{12}(h, p)N^{14}$ reactions, carried out systematically with varying helion incident energy, have demonstrated again that the reaction mechanism is complex, having both direct and compound amplitudes. Of particular interest, has been the demonstration of striking resonant behavior and selective population of individual magnetic substates of the residual nuclear levels. We suggest that these phenomena result from the presence of quasigiant resonances, at high compound-system energies, which have simple structure corresponding to single protons coupled to the excited, residual-core nucleus. These configurations distribute their strength over a large number of underlying complex compound-nucleus levels, with a distribution width ~0.5–1.0 MeV to yield the observed resonant phenomena in the partial cross sections. A correlation has been noted in the experimental data between population of $|m|=1$ substates in the residual nucleus and backward peaking in the corresponding proton angular distributions. We suggest a very crude description of this phenomenon.

Of particular interest will be the determination of whether these observed effects are of general occurrence or whether we have accidentally come upon a particularly favorable case. Measurements to this end are in progress in this laboratory.

ACKNOWLEDGMENTS

We are much indebted to D. Kurath, H. A. Weidenmuller, and J. Ginnochio for illuminating discussions concerning this work and to Dr. Kurath for providing us with his two-particle fractional parentage coefficients and the wave function for C^{12} based on the Cohen-Kurath model. One of the authors (D.A.B.) wishes to express his appreciation to Professor S. Gorodetzky for the hospitality extended to him at the Institut de Recherches Nucléaires, Strasbourg.

[18] N. Stein, C. A. Whitten, Jr., and D. A. Bromley, Phys. Rev. Letters **20**, 113 (1968).